Frontiers of Information Technology & Electronic Engineering
www.jzus.zju.edu.cn; engineering.cae.cn; www.springerlink.com
ISSN 2095-9184 (print); ISSN 2095-9230 (online)
E-mail: jzus@zju.edu.cn

Review:

Recent progress on the applications of micro/nanofibers in ultrafast optics*#

Xinying HE[1], Yuhang LI[2], Zhuning WANG[1], Sijie PIAN[1], Xu LIU[1], Yaoguang MA†‡[1]

[1]*State Key Laboratory for Extreme Photonics and Instrumentation, College of Optical Science and Engineering, Intelligent Optics and Photonics Research Center, Jiaxing Research Institute, ZJU–Hangzhou Global Scientific and Technological Innovation Center, International Research Center for Advanced Photonics, Zhejiang University, Hangzhou 310027, China*

[2]*State Key Laboratory of Precision Measurement Technology and Instruments, Department of Precision Instrument, Tsinghua University, Beijing 100084, China*

†E-mail: mayaoguang@zju.edu.cn

Received July 29, 2023; Revision accepted Nov. 27, 2023; Crosschecked Aug. 6, 2024

Abstract: Ultrafast fiber lasers are indispensable components in the field of ultrafast optics, and their continuous performance advancements are driving the progress of this exciting discipline. Micro/Nanofibers (MNFs) possess unique properties, such as a large fractional evanescent field, flexible and controllable dispersion, and high nonlinearity, making them highly valuable for generating ultrashort pulses. Particularly, in tasks involving mode-locking and dispersion and nonlinearity management, MNFs provide an excellent platform for investigating intriguing nonlinear dynamics and related phenomena, thereby promoting the advancement of ultrafast fiber lasers. In this paper, we present an introduction to the mode evolution and characteristics of MNFs followed by a comprehensive review of recent advances in using MNFs for ultrafast optics applications including evanescent field modulation and control, dispersion and nonlinear management techniques, and nonlinear dynamical phenomenon exploration. Finally, we discuss the potential application prospects of MNFs in the realm of ultrafast optics.

Key words: Micro/Nanofibers (MNFs); Nonlinear dynamics; Dispersion; Ultrafast optics
https://doi.org/10.1631/FITEE.2300509 **CLC number:** TN253; TN241

1 Introduction

The rapid pace of scientific exploration and industrial advancement requires ultrafast lasers with higher pulse energy, shorter pulse duration, and more importantly, a better understanding of the physics and mechanisms of power-scalable mode-locking and controllable intrapulse phase dynamics (Shi, 2022). Micro/Nanofibers (MNFs), which are novel optical fibers with controllable dispersion and nonlinearity, have emerged as a constantly growing research platform for mesoscale optics and ultrafast laser dynamics (Tong et al., 2004; Zhang XL et al., 2012; Li W et al., 2014; Lou et al., 2014; Liu M et al., 2015; Li Y et al., 2016; Cai et al., 2017; Li YH et al., 2019; Huang L et al., 2021). Dispersion, along with its interplay with nonlinearity, is a crucial factor that influences pulse dynamics in mode-locked fiber lasers and can reshape the pulse in the time domain and spectrum (Walmsley et al., 2001; Woodward, 2018). Controlling the dispersion characteristics of traditional single-mode fibers (SMFs) is challenging due to the predominance of material dispersion.

‡ Corresponding author
* Project supported by the STI 2030–Major Projects, China (No. 2021ZD0200401), the National Key Research and Development Program of China (No. 2023YFF0613000), the National Natural Science Foundation of China (Nos. 62222511 and 62175122), and the Natural Science Foundation of Zhejiang Province, China (No. LR22F050006)
# Electronic supplementary materials: The online version of this article (https://doi.org/10.1631/FITEE.2300509) contains supplementary materials, which are available to authorized users
ORCID: Xinying HE, https://orcid.org/0009-0008-2239-1264; Yaoguang MA, https://orcid.org/0000-0002-8091-611X

However, in MNFs, waveguide dispersion associated with the structural parameters of the fibers dominates, offering the opportunity for convenient dispersion regulation. Moreover, MNFs provide more compact structures and footprints when used for dispersion compensation (Li YH et al., 2019). MNFs also exhibit a large fractional evanescent field which can be conveniently coupled to nanomaterials decorated on the fiber's surface and greatly strengthen the light–matter interaction. These advantages have led to numerous studies on MNF-based sensors (Spillane et al., 2008; Shan et al., 2013; Lou et al., 2014; Talataisong et al., 2018; Li YP et al., 2019) and MNF-based saturated absorbers for mode-locked lasers (Luo ZC et al., 2018; Liu M et al., 2020).

The generation of an ultrashort pulse has promoted research on nonlinear dynamics and provides a powerful tool to manipulate the operating state of lasers (Huang L et al., 2021). An essential component of nonlinear dynamics is soliton dynamics. Attaining control over dispersion is essential for steering nonlinear soliton dynamics (Billet et al., 2014). For example, self-similaritons generated by the interaction of self-phase modulation (SPM) and gain in the normal dispersion region can exhibit robustness to wave-breaking under high power conditions. Also, their characteristics of linear chirp and a broad, flat spectrum can lead to efficient pulse compression (Graini and Saouchi, 2022; Lidiya et al., 2022; Zhao et al., 2022). Details of other types of solitons, such as bright, dark, vector, dissipative, polarization domain wall and other experimentally verified optical solitons in fiber lasers can be found in the review by Song YF et al. (2019). Soliton self-frequency shift (SSFS) (Alamgir et al., 2021) and dispersion wave (DW) (Brahms and Travers, 2023) are also attracting much attention and can be used to generate tunable ultrashort pulses. In addition, supercontinuum (SC), which arises from a plethora of optical nonlinearity mechanisms, such as soliton fission, SSFS, four-wave mixing (FWM), and DW, has attracted much interest. The interplay between high nonlinearity, dispersion, birefringence, and other cavity parameters enables the generation of nonlinear dynamics and phenomena. Compared with photonic crystal fibers (PCFs), which are commonly used for research in nonlinear dynamics, MNFs show great potential; not only can the dispersion profile of MNFs be tuned by optimizing their structural parameters, but also the high refractive index contrast of MNFs provides much tighter confinement, leading to much higher nonlinear coefficients and the possibility of using nonlinear coating technology for further enhancement. Both characteristics are beneficial for research on nonlinear dynamics.

The characteristics of MNFs and their applications to ultrafast optics are summarized in Fig. 1. The main factors in ultrafast optics are a large fractional evanescent field, controllable dispersion, and high nonlinearity. A large fractional evanescent field enhances the interaction between light and matter, making it suitable for nanomaterial carriers. In addition to being used as a saturable absorber for mode-locking, MNFs can be used as highly nonlinear elements for studying nonlinear dynamics and phenomena when coated with highly nonlinear materials. Controllable dispersion and high nonlinearity are also crucial characteristics. Dispersion and nonlinearity affect the pulse dynamics inside the cavity, which can be used for mode-locking and the study of nonlinear dynamics. In mode-locking, the laser can operate in different states through the management of dispersion and nonlinearity. Regarding the study of nonlinear dynamics, this article primarily focuses on high-harmonic generation, harmonic mode-locking, generation of noise-like pulses, and SC generation.

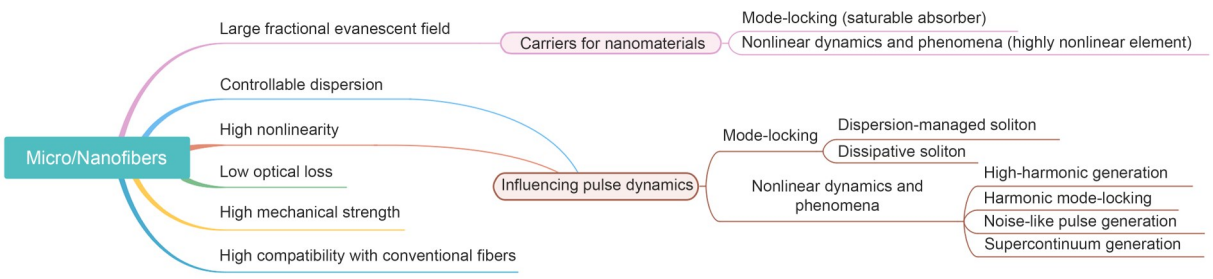

Fig. 1 Characteristics of micro/nanofibers (MNFs) and their applications in ultrafast optics

2 Optical properties of MNFs

Fig. 2a shows our homemade taper-drawing machine for fabricating commercial glass fibers into a specific MNF. The profiles of MNFs obtained from experimental measurement are in excellent agreement with theoretical prediction (Birks and Li, 1992), as depicted in Fig. 2b. Fig. 2c presents a schematic of the fiber tapering. The diameter of the tapered fiber can be monitored in real time by monitoring the transmittance of different wavelengths. The illustration is a photograph of our tiny homemade spectrometer, including a diagram and photograph of the coating.

2.1 Mode evolution of MNFs

The tapering process not only creates a uniform waist region that matches the length of the hot zone but also establishes a taper transition region (Fig. 2c). Within the taper transition region, as the diameter gradually decreases, the characteristics of mode evolution undergo a remarkable transformation. For example, the index of the fundamental mode gradually decreases, which may excite the generation of higher-order modes. However, when the diameter reaches a certain small size, the excited high-order modes are effectively suppressed. They either couple to the air through radiation modes or dissipate entirely, leaving only a few modes. Based on the leaked complicated random interference speckle in the taper transition region, we propose a low-cost (the core components of the spectrometer cost less than $15), scalable spectrum meter that has a picometer resolution and sub-millimeter footprint (Cen et al., 2023) (Fig. 2c, lower right). To comprehensively analyze and understand the transmission characteristics of MNFs, it is essential to consider both the taper transition region with variable diameters and the waist

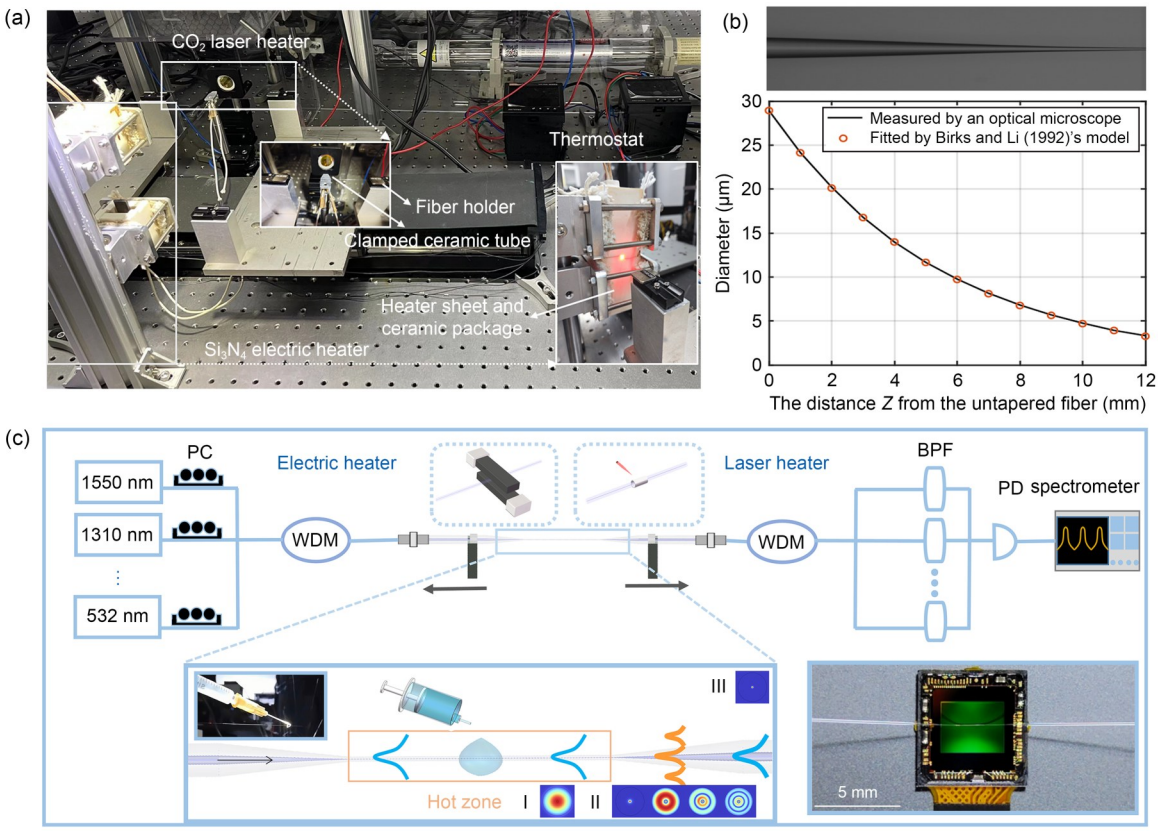

Fig. 2 Schematic of the MNF fabrication system: (a) experimental setup for heat tapering (two heaters are integrated on the same displacement platform; one is a Si_3N_4 electric heater with a long hot zone and high-temperature stability, and the other is a CO_2 laser heater with an ultrashort hot zone); (b) profile of an MNF with a heating zone of 5.5 mm and a 40-mm elongation, and the image of the MNF from an optical microscope; (c) schematic of fiber tapering. The evolution of the mode field at different diameters is also given. The illustration is a photograph of our homemade spectrometer (Cen et al., 2023). PC: polarization controller; BPF: band-pass filter; PD: photodiode; WDM: wavelength division multiplexer

region with uniform diameters (supplementary materials, Section 1).

2.2 Large fractional evanescent field

For MNFs with diameters close to or smaller than the wavelength of light, a large fraction of the energy can be confined within the evanescent field during its propagation along the fiber. The proportion of the evanescent field is influenced by factors such as the material, diameter, and transmission wavelength (Tong et al., 2004). Strong confinement can reduce the mode field area and increase the nonlinear coefficient (Brambilla et al., 2009), so MNFs can be used as carriers of nanomaterials. In ultrafast optics, MNFs coated with nanomaterials can be used as saturation absorbers in mode-locking lasers and highly nonlinear elements in the study of nonlinear dynamics and phenomena.

2.3 Dispersion of MNFs

MNFs offer great potential in the field of ultrafast optics where controlling the dispersion is decisive (Li YH et al., 2019). The dispersion characteristics of MNFs are significantly affected by their diameters (supplementary materials, Section 2).

In ultrafast fiber lasers, the pulse envelope propagates with the group velocity, and the group velocity dispersion determines the width of the pulse and affects the evolution of the pulse in the cavity. The group velocity dispersion (GVD) parameter β_2 of MNFs is shown in Fig. 3a. This diameter-dependent engineering allows for precise control over the dispersion properties of MNFs. By manipulating the diameter of MNFs, it is possible to design the β_2 to be normal, anomalous, or zero. Additionally, the zero dispersion wavelength (ZDW) of MNFs experiences a red shift as the diameter increases, adding another degree of freedom for dispersion control and phase-matching. This becomes especially critical for nonlinear dynamical processes such as SC generation (Stark et al., 2012; Zhang X et al., 2016).

2.4 Nonlinearity of MNFs

For MNFs, the nonlinear refractive index n_2 related to the third-order polarizability is no longer the same in the core and cladding, which makes the nonlinear coefficients of MNFs differ from the standard definition for traditional fibers (Agrawal, 2013):

$$\gamma = \frac{2\pi}{\lambda} \frac{\iint_{-\infty} n_2 |F(x,y)|^4 \mathrm{d}x\mathrm{d}y}{\left(\iint_{-\infty} |F(x,y)|^2 \mathrm{d}x\mathrm{d}y\right)^2}, \tag{1}$$

where $F(x, y)$ is the normalized transverse distribution of the fundamental mode in the core.

Fig. 3b elucidates the remarkable disparity in the nonlinear coefficient γ between MNFs and conventional SMFs (HI1060), showing the potential for MNFs to exhibit orders of magnitude higher nonlinear coefficients. Furthermore, the use of coating technology further augments the already impressive nonlinear characteristics of MNFs, rendering them exceptionally well-suited for the generation and exploration of nonlinear phenomena. In addition, the nonlinear coefficient

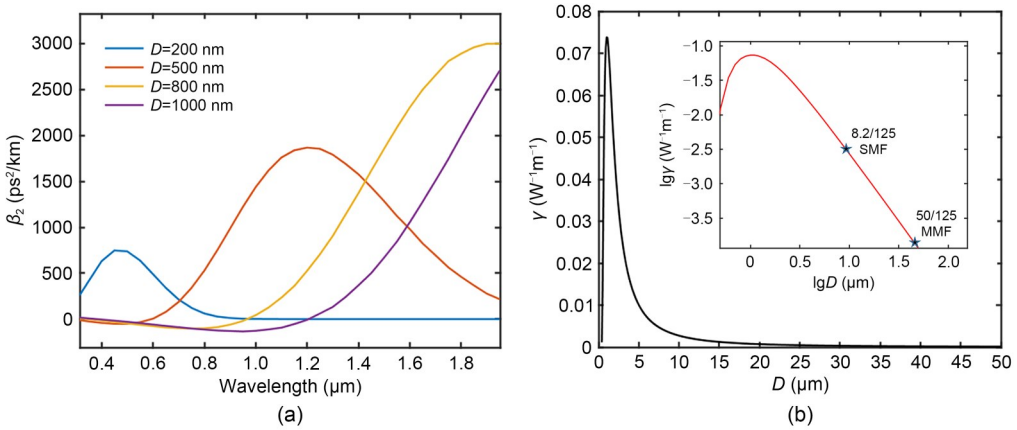

Fig. 3 Characteristics of MNFs: (a) group velocity dispersion of MNFs with different diameters; (b) diameter-dependent γ of MNFs with a wavelength of 1550 nm in linear and log coordinates. The conventional single-mode fiber (SMF) and multimode fiber (MMF) are also displayed for comparison

of MNFs reaches its maximum value when the diameter is about 75% of the transmission wavelength (Foster et al., 2004). Table 1 compares the dispersion and nonlinearity coefficients of different fibers, from which we can see the advantages of MNFs. Note that these comparisons are based on silica fibers, and the use of alternative highly nonlinear materials may yield even higher nonlinear coefficients.

Table 1 Comparison of SMF, MMF, PCF, and MNF (1550 nm)

Fiber type	Dispersion (ps^2/km)	Nonlinear coefficient ($W^{-1}m^{-1}$)	Reference
SMF	−15	3.81e-3	Agrawal (2013)
MMF	−20	1.15e-4	Agrawal (2019)
PCF1	2.17	0.011	Zhang X et al. (2007)
PCF2	−150	0.025	Zhang YC et al. (2021)
MNF (d=1.2 μm)	100	0.07	Zhou J et al. (2021)

In addition to the three main characteristics, the low optical loss, high mechanical strength, and high compatibility with conventional optical fibers are reasons why MNFs have potential applications in ultrafast optics (supplementary materials, Section 3).

Accordingly, benefiting from these characteristics, MNFs serve as an excellent platform for investigating ultrafast optics. For different nonlinear dynamics and phenomena, the requirements for dispersion and nonlinearity distribution in the entire cavity are different. These requirements can be obtained by solving the generalized nonlinear Schrodinger equation (GNLSE) to simulate the dynamic evolution of pulses within the cavity (Agrawal, 2013). The GNLSE is usually solved with a distributed Fourier transform and finite difference method, and the physics-informed neural network is used to predict the complex nonlinear propagation process of pulses (Fang et al., 2022; Jiang XT et al., 2022). Based on the required total dispersion and nonlinearity, the values of dispersion and nonlinearity that the MNFs should provide can be determined. Consequently, MNFs with appropriate structural parameters can be chosen accordingly. Further modification can be achieved through coating, to tailor their dispersion and nonlinearity characteristics.

3 Applications of MNFs in ultrafast optics

3.1 Component of ultrafast optical devices

In the realm of ultrafast optics, innovative strategies to generate ultrashort pulses are being explored, with mode-locking emerging as a crucial factor. The characteristics of MNFs, such as a high fractional evanescent field and diameter-dependent dispersion, make them a crucial component of passively mode-locked lasers.

3.1.1 Evanescent field modulation and control

Benefiting from a strong or rapid near-field interaction between light and nanomaterials, the nonlinearity of MNFs decorated with nanomaterials could be enhanced (Zhang H et al., 2012; Duan et al., 2015; He et al., 2016). Therefore, this composite structure can be exploited as a saturated absorber to generate ultrashort pulses (Luo ZC et al., 2018; Li YH et al., 2019; Liu M et al., 2020; Wang LZ et al., 2020) and provide advantages over nanomaterials alone, such as a high optical damage threshold (Liu M et al., 2020). The commonly used nanomaterials include graphene (He et al., 2016; Liu XM et al., 2016; Yang G et al., 2016; Cai et al., 2017; Wu et al., 2022), MXenes (Ahmad et al., 2021), topological insulators (Ahmad et al., 2022), and quantum dots (Du et al., 2017). Further information can be found in Li YH et al. (2019) and Liu M et al. (2020). In addition, the photo-thermal effect via the evanescent field along the MNFs could be greatly enhanced (Wang YD et al., 2016). By incorporating graphene on the surface of MNFs, the effective nonlinear index can be modified. Because the heat generated in graphene transfers to MNFs, the graphene-decorated MNF becomes an effective tool for dynamically controlling the phase shift in ultrafast fiber lasers. Chen WB et al. (2023) increased the thermal nonlinearity of graphene-decorated microfibers (GMFs) and the nonlinear phase shift difference between two counter-propagating beams by increasing the control laser power. This affects the self-starting performance of the laser, and the mode-locked threshold is linearly decreased, as shown in Fig. 4a. The self-starting mode-locked threshold of the figure-9 fiber laser can be attained in a flexible pump power range. After achieving stable mode-locking operation, the output power of the mode-locked pulses can be adjusted when the

control laser is turned on again, due to the difference in the nonlinear phase shift. The output power may either decrease linearly (as shown in Fig. 4b) or initially increase and then decrease, depending on the initial mode-locking state. To improve the speed of the phase shift difference control, the Kerr effect can be used to achieve faster control of the phase shift difference, and the ultrafast laser can be used as the control laser.

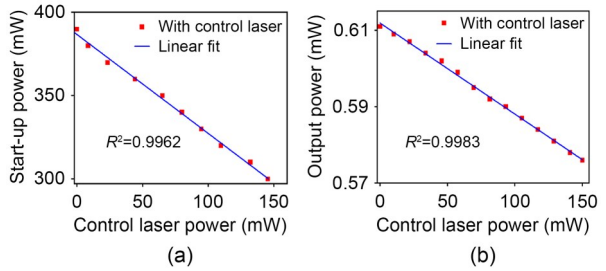

Fig. 4 Mode-locking of a figure-9 fiber laser based on thermal nonlinearity of graphene-decorated MNF: (a) start-up power at different control laser powers; (b) output power with different control laser powers after the mode-locked operation (Chen WB et al., 2023)

The evanescent field provides a platform well-suited for coupling and interference between different modes, enabling MNFs to function as a polarization beam splitter (PBS) or polarizer due to the differences in optical paths among the modes.

Zhang ZS et al. (2015) obtained a polarizer based on MNFs by precisely controlling the partial overlap of two MNFs with equal length. Benefiting from the asymmetric transverse cross-section of the polarizer and large fractional evanescent field of MNFs, the overlapping region exhibits significant birefringence, forming an effective polarizer. The transmission spectrum can be adjusted by altering the diameter of the MNFs and the length of the overlapping region. However, the fabrication of this polarizer involves rather delicate manipulation of equal length cleaving and precise stacking of the MNFs. To simplify the construction, Zhou XB et al. (2021) proposed an all-fiber PBS composed of two parallel coupled microfibers. They considered that there are two different polarization states (TE and TM modes), each with a symmetrical supermode (even mode) and an antisymmetrical supermode (odd mode). Due to the interference between the symmetric TE mode and antisymmetric TM mode, the energy of the light was coupled to adjacent optical fibers through the evanescent field. When the length of the coupling region and the diameter of the MNF are proper, the TE and TM modes would be separated. The characteristics of the MNF-based PBS at 1.5 μm wavelength bands are depicted in Fig. 5. Soliton outputs were obtained experimentally. Zhou XB et al. (2021) pointed out that the birefringence effect increases with a decreasing fiber diameter. Therefore, the oscillation period of the polarization extinction ratio (PER) with respect to wavelength decreases with a decreasing fiber diameter of MNFs, which can affect the selection of diameter.

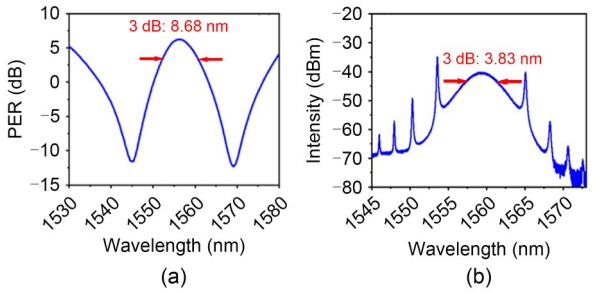

Fig. 5 Mode-locked all-fiber laser based on MNF polarization beam splitter: (a) polarization extinction ratio (PER) spectra at the 1.5 μm band; (b) spectrum of the mode-locked fiber laser at 1.5 μm (Zhou XB et al., 2021)

3.1.2 Dispersion and nonlinearity management

Dispersion and nonlinearity in the cavity play vital roles in pulse shaping and spectrum optimization in ultrafast lasers (Woodward, 2018). When a pulse transmits in MNFs, due to the small mode field area (MFA), it is easy to generate high power density, so nonlinear effects cannot be ignored. These nonlinear effects cause significant nonlinear phase accumulation, leading to pulse splitting, and limit the peak power of the ultrafast fiber laser. To balance or suppress these nonlinear effects, increasing the MFA to reduce the nonlinear coefficient is an effective approach. As a result, PCFs with large MFAs are rapidly being developed (Ranka et al., 2000; Akimov et al., 2003). Another solution is to manage the dispersion and nonlinearity, and MNFs are an attractive option in this regard.

There are two main advantages of using MNFs for dispersion and nonlinearity management. First, compared with dispersion compensation elements in free space (such as grating pairs), MNFs have compact and all-optical fiber structures. Second, MNFs have large and diameter-dependent dispersion, so the

dispersion can be compensated for accurately by tailoring their diameters. By managing the dispersion using MNFs, a laser can operate in a dispersion-managed soliton (Wang LZ et al., 2018; Yang PL et al., 2018) or a dissipative soliton (Li YH et al., 2018). A typical dispersion-managed mode-locked laser is described in Fig. 6. The MNF in the cavity is the dispersion delay line for dispersion compensation, and the MNF outside the cavity achieves further pulse compression.

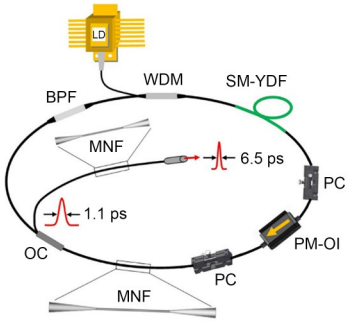

Fig. 6 Schematic of a typical dispersion-managed mode-locked laser (Yang PL et al., 2018). LD: laser diode; PC: polarization controller; WDM: wavelength division multiplexer; SM-YDF: single-mode ytterbium-doped fiber; OC: optical coupler; PM-OI: polarization-maintaining optical isolator; BPF: band-pass filter

The operating state of lasers is determined by the total dispersion within the entire cavity. In other words, when a specific output pulse is required, the dispersion that needs to be compensated for is deduced by the total dispersion required for the entire cavity. By considering the relationship between the dispersion and the diameter of MNFs, the structural parameters of the MNFs can be determined. More detailed information on the applications of MNFs in mode-locked lasers can be found in the literature (Li YH et al., 2019; Wang LZ et al., 2019; Liu M et al., 2020).

3.2 A platform for nonlinear phenomena and dynamics

Nonlinearity is a requirement for passive mode-locking, but too high nonlinearity can lead to pulse splitting and limit the output power. However, an appropriate level of nonlinearity can stimulate various nonlinear phenomena in mode-locked fiber lasers. Thus, MNFs with high nonlinearity provide an ideal platform for exploring nonlinear dynamics. Meanwhile, the study of nonlinear dynamics will promote the improvement of the performance of mode-locked fiber lasers (Grelu and Akhmediev, 2012; Liu M et al., 2020).

3.2.1 High-harmonic generation

The diameter-dependent dispersion characteristic of MNFs is suitable for parametric processes that require phase matching. Among these processes, the generation of high-order harmonics stands out, providing a convenient and efficient means of producing light of different wavelengths.

Grubsky and Savchenko (2005) derived a mathematical model of the third-harmonic generation (THG) in MNFs and provided an expression of the conversion efficiency of THG, as shown in Eq. (2):

$$\frac{P_3}{P_0}=2\left(n_2|J_3|P_0\right)^2\left(\frac{k_0}{\Delta\beta}\right)^2, \tag{2}$$

where P_0 and P_3 are the input fundamental wave power and the third-harmonic power respectively, J_3 is the nonlinear overlapping integral between P_0 and P_3, k_0 is the propagation constant of the fundamental wave in vacuum, and $\Delta\beta=\beta_3-3\beta_1$ is the propagation constant mismatch.

Eq. (2) shows that the improvement of THG conversion efficiency can be generally considered from the following aspects: reducing the phase mismatch; selecting a third-order mode with a large overlapping integral with the fundamental mode; choosing materials with a large nonlinear refractive index n_2. For MNFs, any mode of the third-harmonic wave, other than its fundamental mode $\mathrm{HE}_{11}(3\omega)$, can be phase-matched with the fundamental mode of the fundamental wave $\mathrm{HE}_{11}(\omega)$ by selecting an appropriate diameter, and the most efficient overlap is between $\mathrm{HE}_{11}(\omega)$ and $\mathrm{HE}_{12}(3\omega)$. Grubsky and Feinberg (2007) achieved an experimental conversion efficiency of 2×10^{-6} which is three times lower than the theoretical value obtained from Eq. (2), using MNF with a diameter of about 0.49 μm and an effective length of 100 μm. They attributed the difference to slight diameter variations and not the optimal diameter. The conversion efficiency can be further improved when using longer MNFs, and the efficiency will reach 90% possibly in a 5 cm MNF, but the inherent non-uniformities of MNFs along the length make it difficult to achieve such high efficiency in practice.

Nonadiabatic transmission of HTG in the high-order modes can deteriorate the conversion efficiency and third-harmonic quality. Therefore, Ha et al. (2021) reduced the diameter of the cladding by introducing wet etching before fiber tapering and obtained an MNF that allowed simultaneous adiabatic transmission of multiple high-order modes and fundamental modes. Adiabatic transmission requires that the effective refractive index of high-order modes be distinguished. However, in the traditional tapering process, high-order modes become cladding modes, causing their effective refractive indices to become very similar. MNFs that support the simultaneous adiabatic transmission of different modes provide a good platform for THG. Ha et al. (2021) obtained an improved third-harmonic conversion efficiency of 1.5×10^{-4} by using a 10-mm MNF drawn from a 17-μm-thick cladding-etched fiber. They pointed out that the conversion efficiency could be further improved by increasing the length of the waist and improving the surface uniformity of MNFs.

Although Grubsky and Feinberg (2007) pointed out that phase mismatches included not only linear mismatches caused by the refractive index but also nonlinear mismatches caused by the nonlinear effects such as SPM and cross-phase modulation (XPM), they did not consider the nonlinear term in their practical calculations. Therefore, the conversion efficiency obtained by experiment is much lower than that in theory. Considering the nonlinear phase mismatch term, Jiang XJ et al. (2018) took the diameter, length, and pump power of MNFs into consideration for iterative adaptive optimization to reduce the total phase mismatch, and achieved a conversion efficiency of several percent at peak pump powers lower than 2000 W with an MNF several centimeters long.

To further improve the efficiency of THG, Jiang XJ et al. (2017) introduced a method that involved a counter-propagating pulse train. The forward pump light was periodically modulated with the help of quasi-phase-matching technology. The forward pump light can be regarded as quasi-CW, and the counter-propagating pulse train and the forward pumping light met at every other coherence length L_c. That is, in the region satisfying the phase matching, a counter-propagating optical field did not exist, and in the region not satisfying the phase matching, a counter-propagating field existed and made the harmonic intensity zero, avoiding the transfer of harmonic energy to the pump. With this scheme, they further improved the conversion efficiency. They pointed out that the output harmonic power could be enhanced by several orders of magnitude by optimizing the parameters of the MNFs and input pulse.

In addition to THG, the generation of higher harmonics is expected. However, due to the limitation of high-order nonlinear polarizability, the generation of higher-order harmonics is usually realized by a cascade scheme. MNFs offer the potential for phase-matched FWM by carefully controlling their dispersion, so they are suitable for cascade schemes for higher-order harmonics generation. The fourth harmonic (FH) and fifth harmonic (5H) in two MNFs using the FWM effect were achieved by Khudus et al. (2016).

In summary, in the generation of high-order harmonics, the controllable dispersion of MNFs plays a crucial role in phase matching. To achieve high conversion efficiency in high-order harmonic generation, it is necessary to minimize the phase mismatch between the fundamental mode and the harmonics. Additionally, further improvement in conversion efficiency can be achieved by using the nonlinear mismatch.

3.2.2 Harmonic mode-locking

Ultrafast lasers with high repetition rate (HRR) have great prospects in optical communication (Keller, 2003), micromachining (Yoshino, 2008; Kalaycıoğlu et al., 2018), and other applications (Song DH et al., 2021). The common techniques used to achieve an HRR are to shorten the cavity length and use harmonic mode-locking (HML). Compared to simply shortening the cavity length, HML offers more flexibility and higher repetition rates. When the pump power is sufficient or the nonlinearity accumulated in the cavity is high enough, multiple pulses can propagate simultaneously in the cavity, achieving the state of HML. Consequently, some MNFs decorated with highly nonlinear nanomaterials have been proven to generate high-order harmonics with repetition rates up to GHz (Liu M et al., 2014; Bogusławski et al., 2019; Wang ZH et al., 2019). Numerical results show that dispersion waves gain depletion and recovery, and acoustic waves play crucial roles in the formation of HML during the early, middle, and later stages. The final stabilization of the HML state is achieved through acoustic resonance, which can capture pulses at a fixed temporal

position (Liu XM and Pang, 2019). Acoustic resonance has discrete intrinsic frequencies and different gain factors which depend on the excitation mode and the diameter of the fiber. The small gain factor in SMF results in an unstable repetition rate and large pulse timing jitter (Kang MS et al., 2008). An MNF with a strong acoustic resonance effect is a more suitable scheme. MNFs of different diameters support different acoustic modes and thus have different acoustic frequencies. By designing the diameter, the acoustic frequency can be flexibly controlled (Cao et al., 2019). Huang L et al. (2020) realized high-order HML of 2.3828 GHz and 1.7852 GHz by using an MNF with a waist length of 16 cm and a waist diameter of 1.56 μm, respectively. The repetition rates match well with the frequencies of R01 and TR21 acoustic modes, and this HML laser has high stability. An HML based on nonlinear multimode interference has been proposed (Nazemosadat and Mafi, 2013). This nonlinear saturable absorption mechanism is realized by changing the coupling efficiency from multimode fiber (MMF) to SMF by controlling the incident optical power and has the advantages of being independent of the polarization state and a high damage threshold. Wang RY et al. (2022) proposed a novel HML fiber laser based on a tapered SMF–MMF–SMF ultrafast optical switch, as shown in Fig. 7. As the diameter decreases, the self-imaging period is reduced, the dependence of nonlinear multimode interference mode-locking on the length of MMF is eliminated, and the nonlinear coefficients are improved, so the tapered SMF can easily achieve mode-locking operation. Fig. 7 shows that the pump power is linearly correlated with the harmonic order, and the harmonic order for a diameter of 15 μm is higher than that for diameters of 30 μm and 40 μm under the same pump power.

Generally, achieving a higher stability and repetition rate (>10 GHz) in a high-power HML can be attained by using a longer uniform waist and a smaller waist diameter, respectively.

Dissipative four-wave mixing (DFWM) is a new scheme of mode-locking where the mode-locking pulse is obtained by adding multi-wavelength selective elements (such as comb filters) into the cavity and managing dispersion and nonlinearity (Li AZ et al., 2019; Zhou XF et al., 2022). The presence of the comb filter results in the growth of only a few modes, which transfer

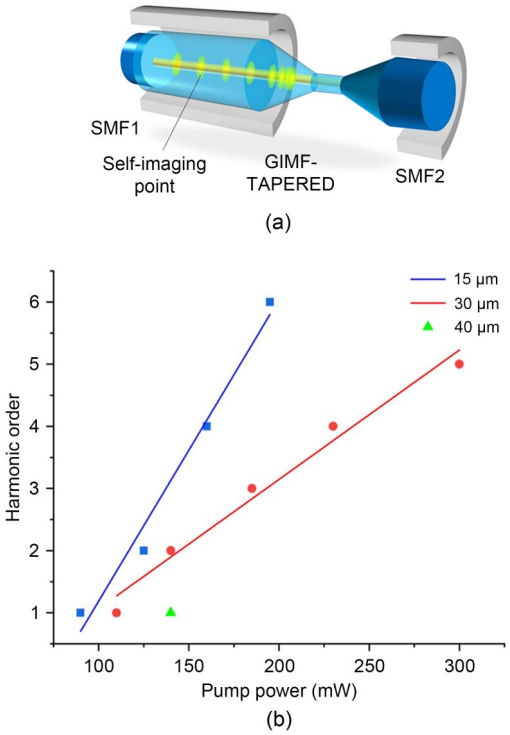

Fig. 7 Harmonic mode-locked fiber laser based on a single-mode fiber (SMF) ultrafast optical switch: (a) schematic of the tapered SMF structure; (b) relationship between pump power and harmonic order at different waist diameters of tapered SMF (Wang RY et al., 2022)

their energy to higher-order modes (the modes far from the center of the band-pass filter) by FWM. Due to the nature of the FWM process, all modes have a constant phase relationship, all sidebands are phase-locked, and the DFWM mode-locking can generate an ultra HRR (up to THz) (Schröder et al., 2009). The existence of the evanescent field provides the possibility of interference between different modes, so a knot resonator composed of MNFs can be used as a comb filter. Wang TQ et al. (2022) used this filter by combining a graphene film to increase the nonlinearity and finally achieved adjustable higher harmonic mode-locked output. The diameter of the MNF knot resonator (MKR) can be altered to change the repetition rate. They obtained a repetition frequency of 323 GHz using an MKR diameter of 200 μm (Figs. 8a and 8b). To further improve the repetition frequency, they adjusted the polarization controller. By adjusting the polarization state, two main peaks appeared, which further increased the repetition rate (Figs. 8c and 8d). They finally obtained a maximum repetition rate of 1.38 THz with the Lyot

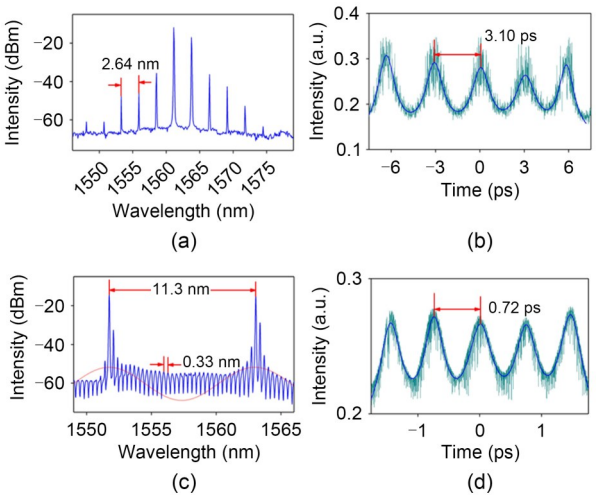

Fig. 8 Experimental results of the harmonic mode-locking with a micro-fiber knot resonator and Lyot filter: the spectra (a) and autocorrelation (b) traces with an MKR diameter of 200 μm; the spectra (c) and autocorrelation (d) traces with an MKR diameter of 1.6 mm after adjusting polarization states (Wang TQ et al., 2022)

filtering effect and pointed out that the harmonic order equals the integer ratio of the free spectral range of the Lyot filter and MKR comb filter.

High-order harmonic mode-locking is obtained when the nonlinearity in the cavity is large. If the nonlinearity in the cavity continues to increase, unique multi-pulse patterns such as noise-like pulses (NLPs) and soliton rain may emerge (Huang QQ et al., 2021).

3.2.3 Noise-like pulse generation

NLPs arouse great interest due to their excellent properties of a broadband smooth spectrum and high pulse energy (Horowitz et al., 1997). In the net anomalous dispersion region, Tang et al. (2005) showed that NLPs are caused by the soliton collapse effect and the positive feedback in the cavity through numerical calculations. In areas of net normal dispersion, traditional soliton pulses cannot be generated, and the formation of NLPs is due to the amplified dispersion wave and background noise. When the saturable absorber is oversaturated, the sharp increase in gain will cause the pulse peak power to become greater than the dispersive wave or the loss of the background noise. This results in fluctuations and instability of higher-order modes, which in turn results in the formation of NLPs (Jeong et al., 2014). In addition, studies have shown that NLP generation can be regulated through dispersion management and enhancement of nonlinear effects (Kang JU, 2000), which can be achieved by embedding MNFs in the cavity (North and Rochette, 2013; Wang LZ et al., 2018; Li YH et al., 2020). Wang ZH et al. (2018) obtained typical NLPs in the 1.5-μm band using a WS_2-deposited MNF as a saturable absorber. Their experimental results confirmed that the WS_2-deposited MNF is not only an excellent saturated absorber but also a highly nonlinear element in NLP generation. Based on the saturated absorption of a tungsten trioxide/polydimethylsiloxane-clad MNF, Abdul Hadi et al. (2022) generated an NLP with a spectral bandwidth of 22.8 nm, a maximum output power of 24.3 mW, and a repetition rate of 7 MHz. In addition to using coated MNFs, bare MNFs were used to generate NLPs. Zhou J et al. (2021) realized experimentally a wide spectrum NLP with a spectrum range of 1000–1600 nm using an MNF with a diameter of 1.2 μm. The output spectrum from using MNFs with different diameters is shown in Fig. 9a. Simulation results from solving the GNLSE agree well with the experimental results. Fig. 9b verifies the effect of the large nonlinear coefficient of the MNF by comparing the output spectra of SMF and MNF. MNFs with different diameters have different dispersion, and the interplay of dispersion and nonlinearity enabled by MNFs is the key factor for the generation of broadband NLPs.

In the generation of NLPs in optical fibers, both dispersion and nonlinear distribution need to be considered. In terms of dispersion, the pump wavelength is expected to be at the anomalous region near the zero-dispersion wavelength, and the nonlinear coefficient is expected to be as large as possible in terms of nonlinearity. Therefore, it becomes necessary to use simulation to optimize the appropriate parameters for MNFs, achieving a balance between these two aspects.

3.2.4 Supercontinuum generation

The generation of SC is influenced by the reciprocal actions of dispersion and nonlinearity when an ultrashort pulse with high intensity is injected into a highly nonlinear fiber. SPM, XPM, SRS, FWM, and other effects will lead to spectrum broadening. Note that by tailoring their shape, MNFs can fabricate and regulate the generation of SC.

Factors influencing SC generation in MNFs, such as fiber and pump pulse parameters, have been studied

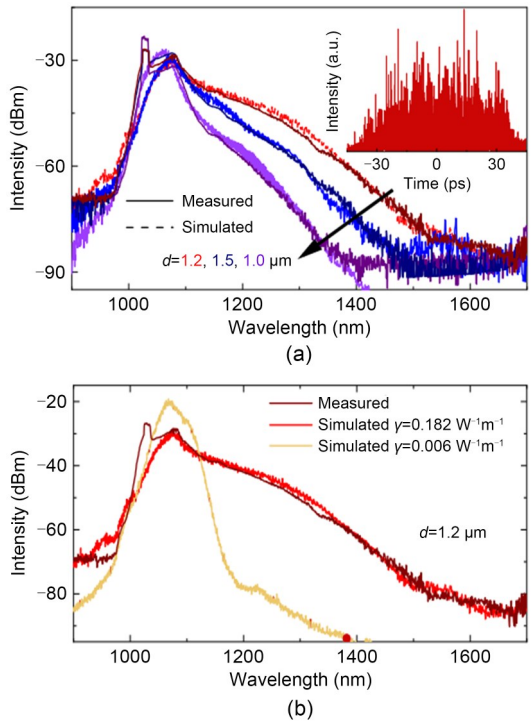

Fig. 9 Broadband spectrum noise-like pulses (NLPs) based on MNFs: (a) simulated and measured spectra for NLPs (the inset shows the simulated waveform with the 1.2-μm MNF); (b) simulated spectra for NLPs for a 1.2-μm MNF, in which the nonlinear coefficient γ is assumed to be 0.182 $W^{-1}m^{-1}$ (SMF) and 0.006 $W^{-1}m^{-1}$ (HI1060). The measurement spectrum (Zhou J et al., 2021) is also shown for comparison

in simulation (Foster et al., 2005; Heidt et al., 2010) and experiment (Birks et al., 2000). In terms of pump pulse parameters, theoretical (Zaytsev et al., 2013) and experimental (Chang et al., 2021; Luo X et al., 2022) studies found that NLPs are effective pumping sources for the generation of SC spectra and are more effective in generating ultra-broadband SC than well-defined pulses (WDPs) (Chang et al., 2023). The femtosecond temporal durations make the peak powers of the inner structures much higher than the peak power of picosecond wave-packets, consequently inducing strong nonlinear optical effects for broadening the spectrum.

With increasing understanding of the SC generation process, attempts are made to generate a flatter and broader spectrum by using dispersion-engineered fibers, in which the dimensions and materials are carefully chosen.

In terms of the dimensions, in addition to selecting the appropriate length and diameter of the waist, the continuous change in the taper diameter along the direction of propagation is attracting increasing attention. The taper offers the advantage of continuously modifying the phase-matching condition, allowing it to be satisfied for a wider range of wavelengths than a waveguide with constant dimensions would allow, making it a promising option for the generation of SC (Zhang R et al., 2004; Chen Z et al., 2010).

In terms of the materials, to further expand an SC to the mid-infrared (MIR) band, chalcogenide MNFs are usually used, and the MIR SC is broadened to a wavelength beyond 5.0 μm (Yeom et al., 2008; Al-Kadry et al., 2014; Wang YY et al., 2018). A broadband SC spectrum extending from 1.5 to 14.5 μm at a −30 dB level has also been obtained by using the designed chalcogenide fiber taper with $AsSe_2$ glass as the core and As_2S_5 glass as the cladding (Saini et al., 2019).

In addition to the tapers obtained from SMFs and PCFs, tapered MMFs are promising avenues for the generation of SC. Periodic self-imaging, which is an important phenomenon in graded index (GRIN) fibers, affects the nonlinear propagation of optical pulses inside (Agrawal, 2019). The taper will accelerate the evolution of spatiotemporal nonlinear dynamics (Fig. 10a). The oscillations experience an acceleration along the propagation direction, and as the diameter decreases, the spacing between the propagation eigenvalues increases, leading to an acceleration in intermodal collisions and energy exchange. The acceleration of intermodal collisions can affect the soliton fission mechanism and the subsequent generation of multimode solitons along with their Cherenkov radiation. In the normal dispersion region, the blue-shifted and red-shifted gain spectral bands progressively drift away from the pump wavelength as the intermodal oscillations speed up, in turn leading to the generation of a markedly flat and uniform spectrum that extends over several octaves with large spectral power densities. As the input pulse travels through the taper section, there is an acceleration of intermodal collisions and newly generated sidebands move away from the pump, thereby sweeping the entire spectrum, resulting in a flat and uniform SC that spans over 2.5 octaves (Fig. 10) (Eftekhar et al., 2019). Some comparison results can be found in Section 4 in the supplementary materials.

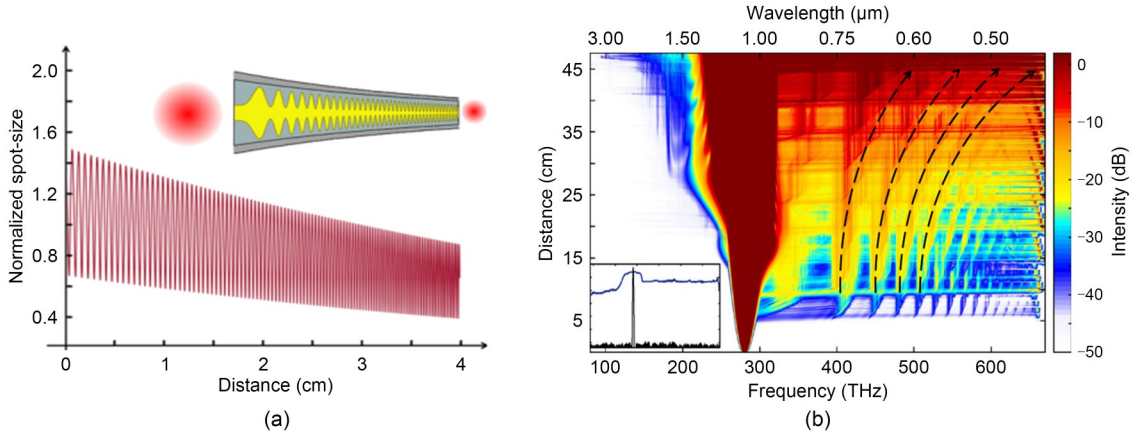

Fig. 10 Supercontinuum generation based on a tapered MMF: the simulation (a) and experimental (b) results from a tapered MMF (Eftekhar et al., 2019)

In general, the generation of SC is a result of multiple nonlinear phenomena. To achieve a broader and flatter SC spectrum, optimizing the shape of MNFs is necessary. In the generation of SC, the number of zero-dispersion wavelengths and the sign and value of dispersion are important. By optimizing the structural parameters, the dispersion and nonlinearity profile can be precisely controlled, further enhancing the performance in the entire spectrum.

4 Conclusions and outlook

In ultrafast optics, MNFs can be used as the main components of mode-locked lasers. They can be used as saturated absorption carriers for nanomaterials and also directly as saturated absorbers and polarizers for mode-locking. Their controllable dispersion and nonlinearity make them ideal for the dispersion and nonlinear management of ultrafast lasers, leading to improved output characteristics. In addition, MNFs present a versatile platform for studying nonlinear dynamics because of their significantly large and customizable nonlinear coefficient. This characteristic allows them to exhibit a variety of nonlinear effects, making them invaluable for research and applications in ultrafast optics. In addition to some of the applications mentioned above, MNFs hold great potential for applications in many other fields. For example, in the field of nonlinear dynamics, MNFs drawn from MMFs with more complex spatiotemporal dynamics (Krupa et al., 2019; Mondal et al., 2020) have not been extensively studied. These complex dynamics offer the potential for a diverse range of nonlinear phenomena. However, the impact of tapering on nonlinear dynamics is not yet fully understood, and more comprehensive studies need to be conducted to better harness nonlinear effects in the future. The coatings and substrates associated with MNFs also need further study, as they play a key role in embellishing or protecting the MNFs. How coatings and substrates will affect the dispersion and nonlinearity properties of the fibers may play a vital role in compact nonlinear systems. Finding new molecules with higher nonlinear coefficients could further strengthen the interaction between the strongly confined light fields and coatings or substrates, which might be a novel way of boosting the performance of MNF-based devices.

Contributors

Xinying HE, Zhuning WANG, and Sijie PIAN investigated the literature and summarized this paper. Xinying HE drafted the paper. Xinying HE, Yuhang LI, Xu LIU, and Yaoguang MA revised and finalized the paper.

Conflict of interest

Yaoguang MA is a corresponding expert of *Frontiers of Information Technology & Electronic Engineering*, and he was not involved with the peer review process of this paper. All the authors declare that they have no conflict of interest.

References

Abdul Hadi MAW, Muhammad FD, Mohd Yusoff N, et al., 2022. Noise-like pulse generation with tungsten trioxide/polydimethylsiloxane-clad microfiber saturable absorber. *Micro Opt Technol Lett*, 64(5):972-977. https://doi.org/10.1002/mop.33197

Agrawal GP, 2013. Nonlinear Fiber Optics (5th Ed.). Elsevier, Amsterdam, the Netherlands, p.327-328.

Agrawal GP, 2019. Self-imaging in multimode graded-index fibers and its impact on the nonlinear phenomena. *Opt Fiber Technol*, 50:309-316. https://doi.org/10.1016/j.yofte.2019.04.012

Ahmad H, Ramli R, Ismail NN, et al., 2021. Passively mode locked thulium and thulium/holmium doped fiber lasers using MXene Nb_2C coated microfiber. *Sci Rep*, 11(1): 11652. https://doi.org/10.1038/s41598-021-90978-x

Ahmad H, Hidayah Mansor N, Aisyah Reduan S, et al., 2022. High power passively mode-locked laser with Sb_2Te_3 deposited tapered fiber in Er/Yb doped fiber laser. *Opt Fiber Technol*, 73:103013. https://doi.org/10.1016/j.yofte.2022.103013

Akimov DA, Schmitt M, Maksimenka R, et al., 2003. Supercontinuum generation in a multiple-submicron-core microstructure fiber: toward limiting waveguide enhancement of nonlinear-optical processes. *Appl Phys B*, 77(2-3):299-305. https://doi.org/10.1007/s00340-003-1200-0

Alamgir I, Shamim MHM, Correr W, et al., 2021. Mid-infrared soliton self-frequency shift in chalcogenide glass. *Opt Lett*, 46(21):5513-5516. https://doi.org/10.1364/OL.443848

Al-Kadry A, Amraoui ME, Messaddeq Y, et al., 2014. Two octaves mid-infrared supercontinuum generation in As_2Se_3 microwires. *Opt Expr*, 22(25):31131-31137. https://doi.org/10.1364/OE.22.031131

Billet M, Braud F, Bendahmane A, et al., 2014. Emission of multiple dispersive waves from a single Raman-shifting soliton in an axially-varying optical fiber. *Opt Expr*, 22(21): 25673-25678. https://doi.org/10.1364/OE.22.025673

Birks TA, Li YW, 1992. The shape of fiber tapers. *J Lightw Technol*, 10(4):432-438. https://doi.org/10.1109/50.134196

Birks TA, Wadsworth WJ, Russell PSJ, 2000. Supercontinuum generation in tapered fibers. *Opt Lett*, 25(19):1415-1417. https://doi.org/10.1364/OL.25.001415

Bogusławski J, Soboń G, Zybała R, et al., 2019. Towards an optimum saturable absorber for the multi-gigahertz harmonic mode locking of fiber lasers. *Photon Res*, 7(9):1094-1100. https://doi.org/10.1364/prj.7.001094

Brahms C, Travers JC, 2023. Efficient and compact source of tuneable ultrafast deep ultraviolet laser pulses at 50 kHz repetition rate. *Opt Lett*, 48(1):151-154. https://doi.org/10.1364/OL.480103

Brambilla G, Xu F, Horak P, et al., 2009. Optical fiber nanowires and microwires: fabrication and applications. *Adv Opt Photon*, 1(1):107-161. https://doi.org/10.1364/aop.1.000107

Cai ZR, Liu M, Hu S, et al., 2017. Graphene-decorated microfiber photonic device for generation of rogue waves in a fiber laser. *IEEE J Sel Top Quant Electron*, 23(1):20-25. https://doi.org/10.1109/jstqe.2016.2568741

Cao M, Li HS, Tang M, et al., 2019. Forward stimulated Brillouin scattering in optical nanofibers. *J Opt Soc Am B*, 36(8): 2079-2086. https://doi.org/10.1364/josab.36.002079

Cen QQ, Pian S, Liu XH, et al., 2023. Microtaper leaky-mode spectrometer with picometer resolution. *eLight*, 3(1):9. https://doi.org/10.1186/s43593-023-00041-7

Chang KY, Wang RC, Yu HC, et al., 2021. Ultra-broadband supercontinuum covering a spectrum from visible to mid-infrared generated by high-power and ultrashort noise-like pulses. *Opt Expr*, 29(17):26775-26786. https://doi.org/10.1364/OE.433815

Chang KY, Chen GY, Yu HC, et al., 2023. Generation of supercontinuum covering 520 nm to 2.25 μm by noise-like laser pulses in an integrated all-fiber system. *Opt Commun*, 533: 129281. https://doi.org/10.1016/j.optcom.2023.129281

Chen WB, Li TJ, Tong LY, et al., 2023. Assisting the mode-locking of a figure-9 fiber laser by thermal nonlinearity of graphene-decorated microfiber. *Opt Expr*, 31(2):2902-2910. https://doi.org/10.1364/OE.476673

Chen Z, Ma S, Dutta NK, 2010. An efficient method for supercontinuum generation in dispersion-tailored lead-silicate fiber taper. *Opt Commun*, 283(15):3076-3080. https://doi.org/10.1016/j.optcom.2010.03.055

Du J, Zhang M, Guo Z, et al., 2017. Phosphorene quantum dot saturable absorbers for ultrafast fiber lasers. *Sci Rep*, 7:42357. https://doi.org/10.1038/srep42357

Duan LN, Wang YG, Xu CW, et al., 2015. Passively harmonic mode-locked fiber laser with a high signal-to-noise ratio via evanescent-light deposition of bismuth telluride (Bi_2Te_3) topological insulator based saturable absorber. *IEEE Photon J*, 7(2):1500807. https://doi.org/10.1109/JPHOT.2015.2404315

Eftekhar MA, Sanjabi-Eznaveh Z, Lopez-Aviles HE, et al., 2019. Accelerated nonlinear interactions in graded-index multimode fibers. *Nat Commun*, 10(1):1638. https://doi.org/10.1038/s41467-019-09687-9

Fang Y, Wu GZ, Wen XK, et al., 2022. Predicting certain vector optical solitons via the conservation-law deep-learning method. *Opt Laser Technol*, 155:108428. https://doi.org/10.1016/j.optlastec.2022.108428

Foster MA, Moll KD, Gaeta AL, 2004. Optimal waveguide dimensions for nonlinear interactions. *Opt Expr*, 12(13):2880-2887. https://doi.org/10.1364/opex.12.002880

Foster MA, Dudley JM, Kibler B, et al., 2005. Nonlinear pulse propagation and supercontinuum generation in photonic nanowires: experiment and simulation. *Appl Phys B*, 81(2-3): 363-367. https://doi.org/10.1007/s00340-005-1865-7

Graini L, Saouchi K, 2022. All-optical 2R regenerator based on similariton-induced spectral broadening. *Opt Eng*, 61(2): 026109. https://doi.org/10.1117/1.Oe.61.2.026109

Grelu P, Akhmediev N, 2012. Dissipative solitons for mode-locked lasers. *Nat Photon*, 6(2):84-92. https://doi.org/10.1038/nphoton.2011.345

Grubsky V, Feinberg J, 2007. Phase-matched third-harmonic UV generation using low-order modes in a glass micro-fiber. *Opt Commun*, 274(2):447-450. https://doi.org/10.1016/j.optcom.2007.02.023

Grubsky V, Savchenko A, 2005. Glass micro-fibers for efficient third harmonic generation. *Opt Expr*, 13(18):6798-6806. https://doi.org/10.1364/opex.13.006798

Ha CK, Nam KH, Kang MS, 2021. Efficient harmonic generation in an adiabatic multimode submicron tapered optical fiber. *Commun Phys*, 4(1):173. https://doi.org/10.1038/s42005-021-00677-2

He XY, Xu M, Zhang XC, et al., 2016. A tutorial introduction to graphene-microfiber waveguide and its applications. *Front*

Optoelectron, 9(4):535-543. https://doi.org/10.1007/s12200-016-0541-3

Heidt AM, Hartung A, Bartelt H, et al., 2010. Deep ultraviolet supercontinuum generation in optical nanofibers by femtosecond pulses at 400-nm wavelength. Proc SPIE 7714, Photonic Crystal Fibers IV, p.771407. https://doi.org/10.1117/12.854279

Horowitz M, Barad Y, Silberberg Y, 1997. Noiselike pulses with a broadband spectrum generated from an erbium-doped fiber laser. *Opt Lett*, 22(11):799-801. https://doi.org/10.1364/ol.22.000799

Huang L, Zhang YS, Cui YD, et al., 2020. Microfiber-assisted gigahertz harmonic mode-locking in ultrafast fiber laser. *Opt Lett*, 45(17):4678-4681. https://doi.org/10.1364/OL.399915

Huang L, Zhang YS, Cui YD, 2021. Optomechanical-organized multipulse dynamics in ultrafast fiber laser. *Chin Phys B*, 30(11):114203. https://doi.org/10.1088/1674-1056/abf344

Huang QQ, Dai LL, Rozhin A, et al., 2021. Nonlinearity managed passively harmonic mode-locked Er-doped fiber laser based on carbon nanotube film. *Opt Lett*, 46(11):2638-2641. https://doi.org/10.1364/OL.425898

Jeong Y, Vazquez-Zuniga LA, Lee S, et al., 2014. On the formation of noise-like pulses in fiber ring cavity configurations. *Opt Fiber Technol*, 20(6):575-592. https://doi.org/10.1016/j.yofte.2014.07.004

Jiang XJ, Lee T, He J, et al., 2017. Fundamental-mode third harmonic generation in microfibers by pulse-induced quasi-phase matching. *Opt Expr*, 25(19):22626-22639. https://doi.org/10.1364/OE.25.022626

Jiang XJ, Zhang DD, Lee T, et al., 2018. Optimized microfiber-based third-harmonic generation with adaptive control of phase mismatch. *Opt Lett*, 43(12):2728-2731. https://doi.org/10.1364/OL.43.002728

Jiang XT, Wang DS, Fan QR, et al., 2022. Physics-informed neural network for nonlinear dynamics in fiber optics. *Laser Photon Rev*, 16(9):2100483. https://doi.org/10.1002/lpor.202100483

Kalaycıoğlu H, Elahi P, Akçaalan Ö, et al., 2018. High-repetition-rate ultrafast fiber lasers for material processing. *IEEE J Sel Top Quant Electron*, 24(3):1-12. https://doi.org/10.1109/jstqe.2017.2771745

Kang JU, 2000. Broadband quasi-stationary pulses in mode-locked fiber ring laser. *Opt Commun*, 182(4-6):433-436. https://doi.org/10.1016/s0030-4018(00)00850-6

Kang MS, Brenn A, Wiederhecker GS, et al., 2008. Optical excitation and characterization of gigahertz acoustic resonances in optical fiber tapers. *Appl Phys Lett*, 93(13):13110. https://doi.org/10.1063/1.2995863

Keller U, 2003. Recent developments in compact ultrafast lasers. *Nature*, 424(6950):831-838. https://doi.org/10.1038/nature01938

Khudus MIMA, Lee T, De Lucia F, et al., 2016. All-fiber fourth and fifth harmonic generation from a single source. *Opt Expr*, 24(19):21777-21793. https://doi.org/10.1364/OE.24.021777

Krupa K, Tonello A, Barthélémy A, et al., 2019. Multimode nonlinear fiber optics, a spatiotemporal avenue. *APL Photon*, 4(11):110901. https://doi.org/10.1063/1.5119434

Li AZ, Li WH, Zhang M, et al., 2019. Tm^{3+}-Ho^{3+} codoped tellurite glass microsphere laser in the 1.47 μm wavelength region. *Opt Lett*, 44(3):511-513. https://doi.org/10.1364/OL.44.000511

Li W, Chen BG, Meng C, et al., 2014. Ultrafast all-optical graphene modulator. *Nano Lett*, 14(2):955-959. https://doi.org/10.1021/nl404356t

Li Y, Sun QZ, Xu ZL, et al., 2016. A single longitudinal mode fiber ring laser based on cascaded microfiber knots filter. *IEEE Photon Technol Lett*, 28(20):2172-2175. https://doi.org/10.1109/lpt.2016.2586098

Li YH, Wang LZ, Kang Y, et al., 2018. Microfiber-enabled dissipative soliton fiber laser at 2 μm. *Opt Lett*, 43(24):6105-6108. https://doi.org/10.1364/OL.43.006105

Li YH, Wang LZ, Li LJ, et al., 2019. Optical microfiber-based ultrafast fiber lasers. *Appl Phys B Lasers Opt*, 125(10):192. https://doi.org/10.1007/s00340-019-7303-z

Li YH, Kang Y, Guo X, et al., 2020. Simultaneous generation of ultrabroadband noise-like pulses and intracavity third harmonic at 2 μm. *Opt Lett*, 45(6):1583-1586. https://doi.org/10.1364/OL.384768

Li YP, Xu ZL, Tan SJ, et al., 2019. Recent advances in microfiber sensors for highly sensitive biochemical detection. *J Phys D Appl Phys*, 52(49):493002. https://doi.org/10.1088/1361-6463/ab3d4e

Lidiya AE, Raja RVJ, Srinivasan B, 2022. Generation of high power ultrashort pulses in tapered Yb-doped PCF through self-similar compression. *IEEE J Quant Electron*, 58(5):1-8. https://doi.org/10.1109/jqe.2022.3186728

Liu M, Zheng XW, Qi YL, et al., 2014. Microfiber-based few-layer MoS_2 saturable absorber for 2.5 GHz passively harmonic mode-locked fiber laser. *Opt Expr*, 22(19):22841-22846. https://doi.org/10.1364/OE.22.022841

Liu M, Luo AP, Zheng XW, et al., 2015. Microfiber-based highly nonlinear topological insulator photonic device for the formation of versatile multi-soliton patterns in a fiber laser. *J Lightw Technol*, 33(10):2056-2061. https://doi.org/10.1109/jlt.2015.2396939

Liu M, Wei ZW, Luo AP, et al., 2020. Recent progress on applications of 2D material-decorated microfiber photonic devices in pulse shaping and all-optical signal processing. *Nanophotonics*, 9(9):2641-2671. https://doi.org/10.1515/nanoph-2019-0564

Liu XM, Pang M, 2019. Revealing the buildup dynamics of harmonic mode-locking states in ultrafast lasers. *Laser Photon Rev*, 13(9):1800333. https://doi.org/10.1002/lpor.201800333

Liu XM, Yang HR, Cui YD, et al., 2016. Graphene-clad microfibre saturable absorber for ultrafast fibre lasers. *Sci Rep*, 6:26024. https://doi.org/10.1038/srep26024

Lou JY, Wang YP, Tong LM, 2014. Microfiber optical sensors: a review. *Sensors*, 14(4):5823-5844. https://doi.org/10.3390/s140405823

Luo X, Tang YT, Dong FL, et al., 2022. All-fiber mid-infrared supercontinuum generation pumped by ultra-low repetition rate noise-like pulse mode-locked fiber laser. *J Lightw Technol*, 40(14):4855-4862.

https://doi.org/10.1109/jlt.2022.3170226

Luo ZC, Liu M, Luo AP, et al., 2018. Two-dimensional materials-decorated microfiber devices for pulse generation and shaping in fiber lasers. *Chin Phys B*, 27(9):094215. https://doi.org/10.1088/1674-1056/27/9/094215

Mondal P, Mishra V, Varshney SK, 2020. Nonlinear interactions in multimode optical fibers. *Opt Fiber Technol*, 54:102041. https://doi.org/10.1016/j.yofte.2019.102041

Nazemosadat E, Mafi A, 2013. Nonlinear multimodal interference and saturable absorption using a short graded-index multimode optical fiber. *J Opt Soc Am B*, 30(5):1357-1367. https://doi.org/10.1364/josab.30.001357

North T, Rochette M, 2013. Raman-induced noiselike pulses in a highly nonlinear and dispersive all-fiber ring laser. *Opt Lett*, 38(6):890-892. https://doi.org/10.1364/OL.38.000890

Ranka JK, Windeler RS, Stentz AJ, 2000. Visible continuum generation in air–silica microstructure optical fibers with anomalous dispersion at 800 nm. *Opt Lett*, 25(1):25-27. https://doi.org/10.1364/ol.25.000025

Saini TS, Nguyen HPT, Luo X, et al., 2019. Broadband high-power mid-IR supercontinuum generation in tapered chalcogenide step-index optical fiber. *OSA Contin*, 2(5):1652-1666. https://doi.org/10.1364/osac.2.001652

Schröder J, Vo TD, Eggleton BJ, 2009. Repetition-rate-selective, wavelength-tunable mode-locked laser at up to 640 GHz. *Opt Lett*, 34(24):3902-3904. https://doi.org/10.1364/OL.34.003902

Shan LY, Pauliat G, Vienne G, et al., 2013. Stimulated Raman scattering in the evanescent field of liquid immersed tapered nanofibers. *Appl Phys Lett*, 102(20):201110. https://doi.org/10.1063/1.4807170

Shi KB, 2022. New soliton dynamics revealed in the normal dispersion region. *Light Sci Appl*, 11(1):67. https://doi.org/10.1038/s41377-022-00748-1

Song DH, Yin K, Zhang JH, et al., 2021. A compact ultrafast GHz mode-locked fiber laser for optical sub-sampling. Proc SPIE 12057, 12th Int Conf on Information Optics and Photonics, Article 120571A. https://doi.org/10.1117/12.2604734

Song YF, Shi XJ, Wu CF, et al., 2019. Recent progress of study on optical solitons in fiber lasers. *Appl Phys Rev*, 6(2):021313. https://doi.org/10.1063/1.5091811

Spillane SM, Pati GS, Salit K, et al., 2008. Observation of nonlinear optical interactions of ultralow levels of light in a tapered optical nanofiber embedded in a hot rubidium vapor. *Phys Rev Lett*, 100(23):233602. https://doi.org/10.1103/PhysRevLett.100.233602

Stark SP, Travers JC, Russell PSJ, 2012. Extreme supercontinuum generation to the deep UV. *Opt Lett*, 37(5):770-772. https://doi.org/10.1364/OL.37.000770

Talataisong W, Ismaeel R, Brambilla G, 2018. A review of microfiber-based temperature sensors. *Sensors*, 18(2):461. https://doi.org/10.3390/s18020461

Tang DY, Zhao LM, Zhao B, 2005. Soliton collapse and bunched noise-like pulse generation in a passively mode-locked fiber ring laser. *Opt Expr*, 13(7):2289-2294. https://doi.org/10.1364/opex.13.002289

Tong LM, Lou JY, Mazur E, 2004. Single-mode guiding properties of subwavelength-diameter silica and silicon wire waveguides. *Opt Expr*, 12(6):1025-1035. https://doi.org/10.1364/opex.12.001025

Walmsley I, Waxer L, Dorrer C, 2001. The role of dispersion in ultrafast optics. *Rev Sci Instrum*, 72(1):1-29. https://doi.org/10.1063/1.1330575

Wang LZ, Xu PZ, Li YH, et al., 2018. Femtosecond mode-locked fiber laser at 1 μm via optical microfiber dispersion management. *Sci Rep*, 8(1):4732. https://doi.org/10.1038/s41598-018-23027-9

Wang LZ, Li LJ, Tong LM, 2019. Optical microfibers and their applications in mode-locked fiber lasers. *Acta Opt Sin*, 39(1):0126011 (in Chinese). https://doi.org/10.3788/Aos201939.0126011

Wang LZ, Li JL, Cui YD, et al., 2020. Graphene/α-In_2Se_3 heterostructure for ultrafast nonlinear optical applications. *Opt Mater Expr*, 10(11):2723-2729. https://doi.org/10.1364/ome.405608

Wang RY, Jin L, Wang JZ, et al., 2022. Harmonic mode-locked fiber laser based on microfiber-assisted nonlinear multimode interference. *Chin Opt Lett*, 20(1):010601. https://doi.org/10.3788/col202220.010601

Wang TQ, Li DD, Ren ZY, et al., 2022. Ultra-high harmonic mode-locking with a micro-fiber knot resonator and Lyot filter. *Opt Expr*, 30(9):14770-14781. https://doi.org/10.1364/OE.454243

Wang YD, Gan XT, Zhao CY, et al., 2016. All-optical control of microfiber resonator by graphene's photothermal effect. *Appl Phys Lett*, 108(17):171905. https://doi.org/10.1063/1.4947577

Wang YY, Dai SX, Peng XF, et al., 2018. Mid-infrared supercontinuum generation spanning from 1.9 to 5.7 μm in a chalcogenide fiber taper with ultra-high NA. *Infr Phys Technol*, 88:102-105. https://doi.org/10.1016/j.infrared.2017.09.007

Wang ZH, Wang Z, Liu YG, et al., 2018. Noise-like pulses generated from a passively mode-locked fiber laser with a WS_2 saturable absorber on microfiber. *Laser Phys Lett*, 15(8):085103. https://doi.org/10.1088/1612-202X/aac551

Wang ZH, Li CY, Ye JW, et al., 2019. Generation of harmonic mode-locking of bound solitons in the ultrafast fiber laser with Sb_2Te_3 saturable absorber on microfiber. *Laser Phys Lett*, 16(2):025103. https://doi.org/10.1088/1612-202X/aaf790

Woodward RI, 2018. Dispersion engineering of mode-locked fibre lasers. *J Opt*, 20(3):033002. https://doi.org/10.1088/2040-8986/aaa9f5

Wu JW, Liu GX, Luo ZC, et al., 2022. Wavelength-tunable Q-switched mode-locked multimode fiber laser. Proc Photonics & Electromagnetics Research Symp, p.540-543. https://doi.org/10.1109/piers55526.2022.9793046

Yang G, Liu YG, Wang Z, et al., 2016. Broadband wavelength tunable mode-locked thulium-doped fiber laser operating in the 2 μm region by using a graphene saturable absorber on microfiber. *Laser Phys Lett*, 13(6):065105. https://doi.org/10.1088/1612-2011/13/6/065105

Yang PL, Teng H, Fang SB, et al., 2018. 65-fs Yb-doped all-fiber laser using tapered fiber for nonlinearity and dispersion

management. *Opt Lett*, 43(8):1730-1733. https://doi.org/10.1364/OL.43.001730

Yeom DI, Mägi EC, Lamont MRE, et al., 2008. Low-threshold supercontinuum generation in highly nonlinear chalcogenide nanowires. *Opt Lett*, 33(7):660-662. https://doi.org/10.1364/ol.33.000660

Yoshino F, 2008. Micromachining with a high repetition rate femtosecond fiber laser. *J Laser Micro/Nanoeng*, 3(3):157-162. https://doi.org/10.2961/jlmn.2008.03.0006

Zaytsev A, Lin CH, You YJ, et al., 2013. Supercontinuum generation by noise-like pulses transmitted through normally dispersive standard single-mode fibers. *Opt Expr*, 21(13): 16056-16062. https://doi.org/10.1364/OE.21.016056

Zhang H, Virally S, Bao QL, et al., 2012. *Z*-scan measurement of the nonlinear refractive index of graphene. *Opt Lett*, 37(11): 1856-1858. https://doi.org/10.1364/OL.37.001856

Zhang R, Zhang XP, Meiser D, et al., 2004. Mode and group velocity dispersion evolution in the tapered region of a single-mode tapered fiber. *Opt Expr*, 12(24):5840-5849. https://doi.org/10.1364/opex.12.005840

Zhang X, Ren XM, Xu YZ, et al., 2007. Ultraflat supercontinuum generation in a dispersion-flattened microstructure fiber. *Micro Opt Technol Lett*, 49(5):1062-1064. https://doi.org/10.1002/mop.22362

Zhang X, Hu HY, Li WB, et al., 2016. Supercontinuum generation in dispersion-varying microstructured optical fibers. Proc SPIE 9834, Laser Technology for Defense and Security XII, Article 98340F. https://doi.org/10.1117/12.2222345

Zhang XL, Belal M, Chen GY, et al., 2012. Compact optical microfiber phase modulator. *Opt Lett*, 37(3):320-322. https://doi.org/10.1364/OL.37.000320

Zhang YC, Yuan JH, Wang KR, et al., 2021. Cascaded-tapered silica photonic crystal fiber for supercontinuum generation. *Opt Eng*, 59(12):126107. https://doi.org/10.1117/1.Oe.59.12.126107

Zhang ZS, Gan JL, Yang T, et al., 2015. All-fiber mode-locked laser based on microfiber polarizer. *Opt Lett*, 40(5):784-787. https://doi.org/10.1364/OL.40.000784

Zhao ZH, Jin L, Set SY, et al., 2022. Broadband similariton generation in a mode-locked Yb-doped fiber laser. *Opt Lett*, 47(9):2238-2241. https://doi.org/10.1364/OL.456808

Zhou J, Li YH, Ma YG, et al., 2021. Broadband noise-like pulse generation at 1 μm via dispersion and nonlinearity management. *Opt Lett*, 46(7):1570-1573. https://doi.org/10.1364/OL.420002

Zhou XB, Qiu MW, Qian YH, et al., 2021. Microfiber-based polarization beam splitter and its application for passively mode-locked all-fiber laser. *IEEE J Sel Top Quant Electron*, 27(2): 1-6. https://doi.org/10.1109/JSTQE.2020.3012667

Zhou XF, Chen ZL, Wang YB, et al., 2022. Theoretical analysis of mode evolution in an adiabatically tapered multimode fiber by coupled local mode theory. *Opt Fiber Technol*, 70:102898. https://doi.org/10.1016/j.yofte.2022.102898

List of supplementary materials

1 Theoretical analysis of mode evolution of MNFs
2 Theory of dispersion characteristics of MNFs
3 Other characteristics of MNFs
4 Some comparison results from supercontinuum generation
Fig. S1 Mode evolution and properties of MNFs
Table S1 Comparison of supercontinuum generated by different optical fibers